International Journal of Pharmaceutics 628 (2022) 122327

Contents lists available at ScienceDirect

International Journal of Pharmaceutics

journal homepage: www.elsevier.com/locate/ijpharm

Enhanced skin localization of metronidazole using solid lipid microparticles incorporated into polymeric hydrogels for potential improved of rosacea treatment: An *ex vivo* proof of concept investigation

Sulistiawati, Kadek Saka Dwipayanti, Muhammad Azhar, Latifah Rahman, Ermina Pakki, Achmad Himawan, Andi Dian Permana *

Faculty of Pharmacy, Hasanuddin University, Makassar 90245, Indonesia

ARTICLE INFO

Keywords:
Rosacea
Metronidazole
Solid lipid microparticles
Hydrogel

ABSTRACT

Metronidazole (MNZ) is a nitroimidazole derivative antibiotic that has been generally used in the treatment of rosacea. However, it has low molecular weight and lipophilicity, limiting the effectiveness of MNZ in the topical treatment of rosacea. This study reports an MNZ-loaded solid lipid microparticle (SLM) gel formulation with sustained drug release effects required in the treatment of rosacea. SLM was formulated using the double emulsification method with five different concentrations of glyceryl monostearate (GMS) as a solid lipid used to encapsulate MNZ. All the MNZ-loaded SLM formulas were extensively characterized by various analytical tools. After optimized MNZ-loaded SLM formulation was obtained, then formulated into gel preparation. To obtain a gel formula with good physical characteristics and drug release in the development of topical therapy, the SLM-loaded gel was further evaluated, covering various parameters such as pH, viscosity, rheology, spreadability, extrudability, skin occlusivity, gel strength, permeation and retention ex vivo, as well as hemolysis tests and antioxidant activity. The evaluation results showed that the SLM formulations had desired properties with optimum encapsulation efficiency. Moreover, the gels prepared from carbomer possessed desired characteristics and were found to be hemocompatible. In addition, the gel formula with a carbomer concentration of 1.25 % can provide better drug release with the highest MNZ retention after 24 h of 2.35 ± 0.05 mg. Notably, the formulation of MNZ into SLM and hydrogel did not affect the antioxidant activity. Thus, it can provide continuous drug release, which could potentially be useful in increasing efficacy in rosacea therapy. The results obtained also showed a significant difference ($p < 0.05$) compared to the control formula and other formulas. Therefore, this study has proven a new approach to developing drug delivery systems for rosacea treatment.

1. Introduction

Rosacea is a chronic inflammatory condition that occurs in the skin, especially the centrofacial area (nose, cheeks, chin, and forehead) that affects blood vessels and sebaceous glands (Gonçalves and De Pina, 2017; van Zuuren et al., 2021). This disorder has various risk factors such as environmental, microbial infection, immune dysfunction, and genetics, but the pathophysiology and pathogenesis are not known with certainty (Engin et al., 2017; Rainer et al., 2019; Zhang et al., 2021). Rosacea can affect anyone, but it is more common in people between the ages of 30 and 60, as well as those with Fitzpatrick skin types I-III (Gonçalves and De Pina, 2017; Jabbehdari et al., 2021). In addition, rosacea is also more prone to occur in women than in men, with a ratio of 1.7:1 (Jabbehdari et al., 2021).

The principle of rosacea treatment is to avoid the causative factors and reduce inflammation. One of the main treatments that has been widely used to treat this disease is using antibiotics such as metronidazole (MNZ) (Engin et al., 2017; Weiss and Katta, 2017). MNZ is a nitroimidazole-derived antibiotic that works by inhibiting the growth of various bacteria and parasites (Ceruelos et al., 2019). MNZ has advantages over other antibiotics, making it the most commonly used antibiotic in the last 50 years due to its low drug resistance, well-established safety profile, and negligible adverse response (Miyachi et al., 2022; Tran et al., 2019). In addition, MNZ is known to treat the inflammation in rosacea through anti-inflammatory and immunomodulatory pathways that work against inflammatory lesions (papules and pustules)

* Corresponding author.
E-mail address: andi.dian.permana@farmasi.unhas.ac.id (A.D. Permana).

https://doi.org/10.1016/j.ijpharm.2022.122327
Received 4 September 2022; Received in revised form 16 October 2022; Accepted 17 October 2022
Available online 21 October 2022

(Miyachi et al., 2022). This skin condition that occurs in someone who has rosacea is also very closely related to the presence of reactive oxygen species (ROS). MNZ also has antioxidant properties resulting from neutrophil modulation and acts as a scavenger (Berth-Jones et al., 2020; Miyachi et al., 2022).

Various therapies that can be used in the treatment of rosacea include oral, topical, injection, laser, and light-based therapies, treatments for certain types of rosacea, and treatments for systemic comorbidities. However, oral and topical therapies are more often used for the treatment of the early stages of rosacea disease (Zhang et al., 2021). MNZ is a class I BCS drug which causes MNZ, when given orally, to be more easily absorbed and more easily eliminated, resulting in reduced bioavailability and is considered less effective in the treatment of rosacea (Yu et al., 2014; Zhang et al., 2019). Treatment of MNZ by oral route may also pose a risk of peripheral neuropathy (Hajariwala et al., 2021). Therefore, MNZ via the topical route is considered to be much more effective in delivering the active substance to the target site for an extended period (Kaur and Guleri, 2013).

MNZ has a low molecular weight of 171.15 g/mol and a log p −1.18. Thus, when applied topically to the skin surface, this drug can penetrate the skin but has a low retention time (Yu et al., 2014). Therefore, it is necessary to control the release of the drug to increase its retention time in the skin without releasing it directly into the system. Several approaches have been developed to improve the skin delivery of MNZ, including nanostructured lipid carrier (Shinde et al., 2019) and nanoemulsion (Yu et al., 2014). However, despite the fact that the formulations could improve the transdermal delivery of MNZ, in the rosacea treatment, it is crucial to retain the drug in the skin layers. It has been previously reported that compared to nanoparticles, microparticle systems possessed better skin retention profiles (Permana et al., 2021a). Accordingly, it was hypothesized that the incorporation of MNZ into the microparticle system could improve the skin retention of MNZ. One of the formulations that can be developed is solid lipid microparticles (SLM). SLM is a drug delivery system that is suitable for various routes, especially through the topical route, because it has low toxicity characteristics, is physiologically compatible, biodegradable, occlusive, and has controlled release properties to increase the bioavailability of the active substance (De Caro et al., 2021; Nahum and Domb, 2021; Rahimpour et al., 2016). In addition, SLM can also provide better solubilization and dispersion of active ingredients and can be produced on a large scale at low costs (Nahum and Domb, 2021). Then, to facilitate the administration of SLM, the selection of topical dosage forms needs to be considered. One of the topical dosage forms that can be used is gel.

When compared with other topical preparations, such as creams and ointments, gels can provide better application and stability properties (Patil et al., 2019). Based on research conducted by Rahimpour et al., (2016), the release of tetracycline HCl through SLM, which was made in the form of a gel dosage form, showed a controlled drug release pattern. Ex vivo studies also showed that there was an increase in dermal deposition of tetracycline HCl up to 7 times that of the control formula. Therefore, the gel dosage form was considered as the most suitable system to deliver MNZ.

The gel in its formulation requires a gelling agent that functions as a gelling agent. Carbomer 940 is a strong gelling agent, so it only takes a small concentration to form a gel (Rowe et al., 2009). In addition, compared to other gelling agents, carbomer 940 is a polymer with superior drug release compared to other polymers and is non-toxic, biocompatible, and non-irritating (Patel et al., 2011; Zhang et al., 2020). Based on previous research conducted by Yen et al. (2015), on the use of carbomers in controlling the release of galantamine, it was found that the gelling agent was able to control the release of galantamine by 2 times with an increase in the amount of carbomer concentration used. To the best of our knowledge, this is the first study developing SLM loaded hydrogel to enhance the skin localization of MNZ. In this study, we formulated SLM using glyceryl monostearate (GMS) as a lipid matrix. Furthermore, the SLMs were incorporated into the carbomer-based hydrogel. A proof of concept was carried out in *an ex vivo* study. The results of this study are expected to be a new system that is more effective in treating rosacea.

2. Material and methods

2.1. Materials

Metronidazole (MNZ), Carbomer 940, triethanolamine (TEA), glycerin, and DMDM Hydantoin were obtained from Sigma-Aldrich Pte ltd. (Singapore). Geleol®/glycerol monostearate was kindly provided by Gattefosse Pvt. ltd., France. Other materials were analytical grade.

2.2. Preparation of metronidazole (MNZ) - loaded solid lipid microparticles (SLM)

MNZ-loaded SLM was prepared using the double emulsification method with glyceryl monostearate (GMS) as a matrix-forming lipid. The SLM formulation in this study used five different concentration ratios of GMS: MNZ, namely 1:2, 2:1, 3:1, 4:1, and 5:1 %w/w, respectively marked as SLM 1, SLM 2, SLM 3, SLM 4, and SLM 5. Initially, SLM was prepared by dissolving MNZ in water. Then, the solution was emulsified in chloroform containing lipids and an emulsifier (to form a water-in-oil (W/O) emulsion) in a probe sonicator adjusted at 80 % amplitude with 10 s pulse on and 5 s pulse off for 1 min. The previously prepared w/o emulsion was emulsified again in water containing 1 % poly(vinyl alcohol) (PVA) to form water-in-oil-in-water (W/O/W) in the sonicator probe. After that, the organic solvent in the double emulsion was evaporated by stirring the double emulsion at room temperature for 6 h to form SLM. To produce concentrated SLMs and separate free MNZ from the SLMs, the formulation was centrifuged at 5,000 rpm for 30 min using an Amicon® Ultra Centrifugal Device (Millipore Inc, molecular weight cut-off (MWCO) of 12 kDa). The obtained microparticles were resuspended with 2.5 % w/v PVP before the lyophilization process. After that, to produce dry powder particles, the mixture was transferred to a freeze-dryer for 26 h (Permana et al., 2019).

2.3. Characterization of MNZ-loaded SLM

2.3.1. Particle size and polydispersity index (PDI)

The determination of the size and particle size distribution of the MNZ-loaded SLM formula was analyzed by light scattering technique using Mastersizer 2000® equipment (Malvern Instruments ltd., UK) (Ghaderi et al., 2014; Rahimpour et al., 2016). This measurement was made in three replications.

2.3.2. Entrapment efficiency (EE) and drug loading (DL)

Entrapment efficiency and drug loading of MNZ-loaded SLM were determined using the method according to the method described previously (Wolska and Brach, 2022). The amount of MNZ encapsulated in SLM was determined by dissolving SLM in methanol. The MNZ-loaded SLM suspension that had been prepared was then centrifuged, and the supernatant obtained was analyzed using a UV–vis spectrophotometer at 320 nm. The percentage of EE and DL can be calculated using the equation below.

$$\mathrm{EE}\,(\%) = \frac{W_{\text{total drug}} - W_{\text{free drug}}}{W_{\text{total drug}}} \times 100 \quad (1)$$

$$\mathrm{DL}\,(\%) = \frac{W_{\text{total drug}} - W_{\text{free drug}}}{W_{\text{lipid}}} \times 100 \quad (2)$$

where, $W_{\text{total drug}}$ is the amount of drug added in the formulation, $W_{\text{free drug}}$ is the amount of free drug in the aqueous phase or which is not encapsulated after separation from SLM, and W_{lipid} is the weight of the lipid phase.

2.3.3. Characterization of MNZ-loaded SLM

The surface morphology of the optimized SLM formulation was observed using scanning electron microscopy (SEM) (JEM-1400Plus; JEOL, Tokyo, Japan). Other analyses were also carried out on MNZ and SLM (a mixture of pure drug and lipid), such as differential scanning calorimetry (DSC) and X-ray diffraction (XRD) measurements of MNZ and SLM formula using differential scanning calorimetry (DSC 2920, TA Instruments, Surrey, UK) and X-ray diffractometer (Rigaku Corporation, Kent, UK), respectively. Then, to see the possibility of chemical interactions between the drug and the compounds used in the formulation, an analysis was carried out using a Fourier transform infrared spectrometer (FTIR) (Shimadzu® FTIR-8400) (Permana et al., 2020a).

2.3.4. In vitro drug release study

The release of MNZ from SLM was carried out using the dialysis method with Spectra/Por® 2, MWCO 12,000 to 14,000 (Spectrum Medical Industries, CA, USA) as dialysis membranes. The release profile of MNZ as a free drug and MNZ-loaded SLM was determined by inserting a dialysis membrane containing the formula into 100 mL of phosphate buffer saline (PBS) medium pH 7.4 as a release medium in an orbital shaker at a speed of 10 rpm and a temperature of 37 °C. At certain time intervals, a 1 mL aliquot of the sample was taken and replaced with a fresh release medium. The amount of MNZ drug released from SLM was then analyzed using a UV–vis spectrophotometer with a wavelength of 320 nm. The in vitro drug release kinetics can be calculated using the equation in section 2.4 (Permana et al., 2019).

2.4. Mathematical modeling of drug release kinetic

The dissolution data obtained can be analyzed to determine drug release kinetics both in vitro and ex vivo. There are five mathematical models that can be applied to the release process to determine the most suitable release kinetics, such as the zero-order release equation (ZO), the first order equation (FO), the Higuchi square root equation (H), the Korsmeyer-Peppas equation (KP), and the Hixson-Crowell (HC) square root model (Sulistiawati et al., 2021).

$$ZO : C_t = C_0 + K_0 t \tag{3}$$

$$FO : \ln C_t = \ln C_0 + K_1 t \tag{4}$$

$$H : C_t = K_H \sqrt{t} \tag{5}$$

$$KP : C_t = K_{KP} t^n \tag{6}$$

$$HC : C_t^{1/3} = C_0^{1/3} K_{HC} t \tag{7}$$

Ct represents the concentration of MNZ released at time t, C_0 represents the initial concentration of MNZ in the dissolution medium (t = 0) and K_0, K_1, K_H, K_{KP}, dan K_{HC} represent the release constants zero-order, first-order, Higuchi, Korsmeyer-Peppas, and Hixson-Crowell (Elmas et al., 2020; Sulistiawati et al., 2021). All of the above parameter calculations were processed using DD-solver software (China Pharmaceutical University, Nanjing, China) (Zhang et al., 2010).

2.5. Preparation of SLM-loaded gel

The optimal SLM formulations were then incorporated into gel preparation (details of the composition of the SLM-loaded gel formula can be seen in Table 1). Briefly, the gel was made by dispersing carbomer into distilled water and left to hydrate for one day. After hydration, the carbomer polymer was neutralized with triethanolamine and homogenized using the Ultra-Truax IKA® T18 basic homogenizer (IKA, Campinas, Brazil) at 15,000 rpm for 15 min. Glycerin, DMDM hydantoin, and MNZ-Loaded SLM were then added slowly to the mixture and homogenized again until an evenly distributed SLM-Loaded Gel was obtained.

Table 1
Composition of SLM-loaded gel.

Composition	%Composition (w/w)			
	F1	**F2**	**F3**	**F4**
MNZ-loaded SLM (equivalent 1 % MNZ)	1.28	1.28	1.28	1. 28
Carbomer 940	0,75	1	1,25	1,5
Triethanolamine	1	1,5	1,75	2
Glycerin	15	15	15	15
DMDM Hydantoin	0,1	0,1	0,1	0,1
Distilled water	ad 100	ad 100	ad 100	ad 100

2.6. Characterization of SLM-loaded gel

2.6.1. pH, viscosity and rheological examination

The pH of the SLM-loaded gel formula was determined using a digital pH meter (Horiba Scientific, Kyoto, Japan) with three replications at 25 °C. Prior to measurement, the pH meter was calibrated with the help of a pH 7 buffer solution. Then the electrode was immersed in the gel formula (Dudhipala & Gorre, 2020; Thomas et al., 2019). The viscosity and rheology of the SLM-Loaded Gel formula were determined using a Brookfield viscometer (model RV) at 25 °C, each measured with three replications using spindle 7. In the determination of viscosity, it was measured at a speed of 50 rpm. Meanwhile, for the determination of rheology, the gel was rotated in stages at 5, 10, 20, 50, and 100 rpm (Himawan et al., 2022; Permana et al., 2021b).

2.6.2. Spredability test

The SLM-loaded gel (1 g) was placed between two glass plates (20 × 20 cm). The standard weight of the top glass plate was 125 g. The sample was measured after 1 min, and then 100 g was added to the load until the final weight of the top plate was 525 g. The diameter of the sample was measured with each additional load, and the procedure was repeated three times. Next, the dispersion curve is made by plotting the load against the diameter formed (Aliyah et al., 2021; Permana et al., 2020b).

2.6.3. Extrudability test

The gel extrudability test was carried out by filling 20 g of gel into a collapsible aluminium tube and sealed with crimping at both ends. The tube containing the preparation was then weighed and placed between two clamped glass slides. Next, on a glass slide, a load of 500 g was given, and the tube cap was removed (Dudhipala and Gorre, 2020; Kaur and Ajitha, 2019). This test was carried out in three replications, and extrudability was calculated using the equation:

$$Extrudability(g/cm^2) = Weight\ applied\ to\ extrudegel/Area \tag{8}$$

2.6.4. In vitro skin occlusivity evaluation

The occlusivity of the SLM-loaded gel was evaluated in vitro by weighing each gel formula (250 mg) and applying it to the surface of the Whatman No. 42 filter paper, with a pore size of 2.5 μm (n = 3). The filter paper was used to cover a 100 mL beaker that had been filled with 50 mL distilled water. As a test control, filter paper without gel formula was used. Furthermore, the beakers were stored in an incubator at 32 ± 0.5 °C, and the weight of the system was recorded at specified time intervals (0, 6, 24, and 48 h) (Malik and Kaur, 2018; Permana et al., 2020b). Occlusivity (F_0) is calculated using the following equation:

$$F0 = \frac{W_0 - W_1}{W_0} \times 100 \tag{9}$$

where, W_0 is the water loss from the control and W_1 is the water loss from the gel formula.

2.6.5. Gel strength determination

The strength of the SLM-loaded gel was determined according to

(Algahtani et al., 2020). The 60 g gel sample was put into a 100 mL measuring cup (d = 1.5 in.). Then, the mounted disk (d = 3 cm; thickness = 3 mm) weighing 30 g was deposited on the gel surface. The strength of this SLM-loaded gel was measured as the time (seconds) required for the disc to sink 5 cm from the surface into the gel.

2.6.6. Ex vivo skin permeation and retention studies

The ex vivo skin permeation test used the Franz diffusion cell method with a diffusion area of 4.9 cm^2. This study used skin from the abdomen of rats as a diffusion membrane which was carefully taken and then washed with PBS solution pH 7.4. Washed mouse skin was placed between the donor compartment and the Franz diffusion cell receptor. The receptor compartment with a capacity of 28 mL was filled with PBS solution pH 7.4 and stirred using a magnetic stirrer at a speed of 100 rpm. The temperature was maintained at 37 ± 1 °C. A 1 g gel sample (containing 10 mg MNZ) was introduced into the donor compartment. At certain time intervals (0.25, 0.5, 0.75, 1, 2, 3, 4, 5, 6, 7, 8, and 24 h), 1.5 mL of receptor medium was sampled and replaced with the fresh medium of the same volume in the receptor medium. The MNZ concentration was then analyzed using a UV–vis spectrophotometer (Dynamica, HALO XB-10) with a validated wavelength of 320 nm (Neupane et al., 2020; Permana et al., 2020b). The cumulative drug released was calculated using the equation in section 2.4. The permeation rate of the preparation can also be calculated using Fick's first law equation, equation (10) (Berthet et al., 2020; de Araújo et al., 2021).

$$J(\mu g/cm2/h) = \frac{dM}{S.dt} \quad (10)$$

where, M is the amount of drug absorbed, S is the area of diffusion, and t is the time.

At the end of the permeation study, after 24 h, the retention test was continued. The skin of the used mice was carefully removed from the Franz diffusion cells and washed three times with fresh receptor medium to remove excess formula. The skin was cut into small pieces, and the MNZ retained in the skin was extracted with 20 mL of methanol, then homogenized at 1000 rpm for 15 min. Samples were centrifuged for 30 min at a speed of 5000 rpm. The supernatant obtained was collected and analyzed by UV–vis spectrophotometry (Badie and Abbas, 2018).

2.7. In vitro hemolysis test of MNZ-loaded SLM and SLM-loaded gel

In vitro hemolysis toxicity screening of MNZ-loaded SLM and SLM-loaded gel was carried out following the previously described spectrophotometric method (Enggi et al., 2021; Khurana et al., 2013). Briefly, red blood cells (RBC) obtained from Wistar rats were centrifuged at 2000 rpm for 20 min to separate RBC from plasma. The RBCs were then washed three times with PBS (pH 7.4) and resuspended with PBS to obtain a 10 % (v/v) RBC stock dispersion. A total of 0.1 mL of the tested sample was then added to 0.9 mL of RBC and incubated for 1 h at 37 ± 0.5 °C. After incubation, the samples were centrifuged at 1500 rpm for 10 min. The preparation of positive and negative controls was carried out by adding 0.1 mL of RBC dispersion with 0.9 mL of Solution X-100 (5 % v/v) and 0.9 mL of PBS (pH 7.4), respectively. To determine the content of oxyhemoglobin released, the supernatant from the test sample, positive control, and negative control was analyzed using a UV–vis spectrophotometer at 546 nm (Dynamica, HALO XB-10). The percentage of hemolysis was calculated using the following equation:

$$\text{Hemolysis}\,(\%) = \frac{(\text{OD test sample}) - (\text{OD negative control})}{(\text{OD positive control}) - (\text{OD negative control})} \times 100 \quad (11)$$

2.8. In vitro antioxidant activity

The antioxidant capacities of MNZ, MNZ-loaded SLM and SLM-loaded gel were assessed using 2,2-diphenyl-1-picrylhydrozyl (DPPH) radical and lipid peroxidation method, as described previously (Permana et al., 2020b). In DPPH method, the tested compounds were dissolved in methanol (2.5 mL) in different concentrations. These solutions were mixed with DPPH solution (2.5 mL) and incubated in the dark for 20 min. The absorbances were determined at 520 nm using spectrophotometric. The concentration of the tested compound, which could inhibit 50 % of DPPH, expressed as IC50 was finally determined. In lipid peroxidation method, the emulsion composed of 0.25 g of linoleic acid, 0.25 g of Tween 80 and 20 mL of 20 mM phosphate buffer (pH 7) was mixed with the tested compounds with the same ratio. The mixture was incubated for 6 h at 37 °C. Following this, 0.1 mL of the mixture was mixed with 5 mL of ethanol (75 % v/v), 0.1 mL of 20 mM of ferrous chloride in 100 mM HCl and 0.2 mL of 30 % w/v ammonium thiocyanate, and was incubated for 5 min at 25 °C. Th absorbances were determined at 500 nm using spectrophotometric, and the IC50 values were determined.

2.9. Statistical analysis

Data are presented as mean ± standard deviation (SD). All results obtained were calculated using Microsoft Excel® 2016 (Microsoft Corporation, Redmond, USA). Statistical analysis was performed using IBM® SPSS® Statistics 21.0 (IBM, Armonk, New York, USA). The data obtained were processed in graphs and diagrams using GraphPad Prism® version 5 (GraphPad Software, San Diego, California, USA). The probability level of $p < 0.05$ was considered significant.

3. Results and discussion

3.1. Preparation and optimization of MNZ - loaded SLM

In this study, MNZ-loaded SLM was prepared using the double emulsification method. MNZ is a hydrophilic drug (Shinde et al., 2019). The double emulsification method has become one of the ideal methods in the preparation of SLM containing hydrophilic drugs. This is evidenced by several previous studies that have been described by Mirchandani et al. (2021). Multiple emulsion systems (water-in-oil-in-water, w/o/w) can provide better entrapment of hydrophilic drugs (Akki et al., 2022). In addition, SLM prepared by this method can avoid the partition of hydrophilic drugs that are released from the oil phase to the outer phase (water) during the emulsification process. In order to support this, the drug is packaged with a stabilizer. In this study, 1 % PVA was used as a stabilizer (Dolatabadi et al., 2015; Shi et al., 2011). Then, in a solid lipid microparticle system, in order for the drug to be well encapsulated, the drug must be soluble in the lipid matrix. Based on research by Shinde et al. (2019), glyceryl monostearate (GMS) is a solid lipid that can provide high dissolution of MNZ because GMS has slightly hydrophilic properties with one ester group and two hydroxyl groups, so it can form hydrogen bonds between the groups of GMS and MNZ.

The ratio of lipids to drugs in the preparation of SLM was the main independent factor that could influence the formation of an optimal microstructured solid lipid system (Nabi-Meibodi et al., 2013). Therefore, this study began by evaluating the SLM system based on various characteristic parameters, such as particle size, polydispersity index (PDI), entrapment efficiency (EE), and drug loading (DL). The results of the evaluation can be seen in Table 2. The determination of the particle size of the SLM formula showed that the higher the lipid concentration, the greater the particle size (Fig. 1 (A)). Meanwhile, for PDI, all SLM formulas are in the range of 0.102 – 0.119. The good particle size for topical application is 1 – 3 μm, so the results obtained indicated that SLM 5 did not meet the standardization of optimal SLM for topical drug delivery systems (Rahimpour et al., 2016). In addition, the statistical analysis results also showed significantly different values ($p < 0.05$) between SLM 4 and SLM 5. The smaller the size of a particle, the more the surface area of the particle increases, which causes its solubility to increase. Therefore, the particles are more easily absorbed into the body

Table 2
Results of particle size, PDI, EE, and DL of MNZ-loaded SLM formulation (means ± SD, n = 3, * = p < 0.05).

Formula	GMS: MNZ	Particle Size (μm)	PDI	EE (%)	DL (%)
SLM 1	1: 2	0,98 ± 0.05	0,102 ± 0.018	49.19 ± 2.12	32.09 ± 2.09
SLM 2	2: 1	1.26 ± 0.11	0,112 ± 0.013	58.83 ± 3.21	28.12 ± 1.98
SLM 3	3: 1	1.65 ± 0.14	0,107 ± 0.011	69.94 ± 4.09	29.19 ± 1.77
SLM 4	4: 1	2.69 ± 0.29	0,119 ± 0.014	88.43 ± 3.12	26.34 ± 2.19
SLM 5	5: 1	5.84 ± 0.43*	0,106 ± 0.009	90.31 ± 4.18	24.09 ± 2.87

(Rabima and Sari, 2019). Then, for PDI, it showed that all formulas met the PDI parameter standard, which is < 0.3, with excellent homogeneity (Algul et al., 2018; Kazemi et al., 2014). This also indicated that the SLM system was more stable because only a few particles underwent aggregation (Rabima and Sari, 2019).

The success of the preparation of the SLM system is very dependent on how much the active substance is absorbed into the system. Fig. 1 (B) shows the increased efficiency of drug entrapment into the SLM system and the increased lipid concentration. Statistical analysis showed that the SLM 4 formulation, with an EE value of 88.43 ± 3.12 %, was a formula with a good EE value because it has a significantly different value ($p < 0.05$) from the formulation SLM 1, SLM 2, SLM 3, and not significantly different ($p > 0.05$) from the SLM 5 formula. The lipid concentration used affected the entrapment efficiency produced because the lipid chains play a role in the formation of imperfect crystals so that they can provide a larger space in the crystal that can accommodate more drugs (Soute and Müller, 2007). The higher the EE value produced, the greater the amount of drug that is absorbed into the system (Lv et al., 2018). In addition to the EE value, drug loading (DL) is also a factor in the success of SLM preparation. The results of the DL evaluation can be seen in Table 2, Fig. 1 (B), which showed results that were inversely proportional to the EE value. The EE and DL capacities are closely related to the particle size and the particle formation process of the SLM system. In addition, solid lipid particles also have limited drug loading capacity for hydrophilic drugs (Mu and Holm, 2018).

After conducting several SLM characterization tests above, it was concluded that SLM 4 was the optimal MNZ-loaded SLM formulation. Accordingly, it was continued for further evaluation and preparation of SLM-loaded gel with particle sizes and PDI that meet SLM standards as a drug in overcoming rosacea with a topical drug delivery system and have higher EE and DL values, with values that are not significantly different ($p > 0.05$) from SLM 5. Although the EE and DL values of SLM 5 were larger, they produced a particle size>3 μm.

3.2. Characterizations of MNZ-loaded SLM

The optimal morphology of the MNZ-loaded SLM (SLM 4) was observed using SEM analysis. The results of the analysis showed that the microparticles formed had a spherical and smooth shape (Fig. 2 (D)). This form is a type of good solid lipid microparticle morphology (Oriani et al., 2016). The results of these observations confirm the optimal particle size and size distribution of SLM, which have been obtained previously using the Mastersizer 2000®, with values of 2.69 ± 0.29 μm and 0.119 ± 0.014 for particle size and size distribution, respectively. The spherical morphology of microparticles has the advantage of being able to reduce the occurrence of aggregation, which can affect the surface area of the particles as well as the absorption of particles (Bertoni et al., 2020; Oriani et al., 2016). Then, the interaction between the drug and excipients was observed using FTIR analysis. Fig. 2 (A) shows the FTIR spectrum of MNZ as a free drug and optimal MNZ-loaded SLM. The spectrum confirms that there was no interaction between the active substance and additives in the SLM system that can cause drug degradation, where the MNZ-loaded SLM spectrum still exhibited the same functional groups found in free MNZ. Based on observations, the infrared spectrum of MNZ-loaded SLM was as follows: stretching at 3215 cm^{-1} (for the OH group), 3102 cm^{-1} (C = CH), 1529 cm^{-1} (NO_2/N—O), 1189 cm^{-1} (stretching vibration of a tertiary amine group), 1075 cm^{-1} (C-OH/C—O), and 865 cm^{-1} (C-NO_2).

The solid-state study of the produced SLM was further analyzed using DSC and XRD (spectra can be seen in Fig. 2 (B) and (C), respectively). DSC analysis was carried out to evaluate the thermal profile, crystallization, and possible interactions between drugs and excipients (Agubata et al., 2014; Rahimpour et al., 2016). The DSC profile of MNZ shows an endothermic peak with a melting point at 160 °C, while the profile of MNZ-loaded SLM shows no peak, which means that there was a change in the solid form of MNZ from a crystalline to an amorphous form after encapsulation. The amorphous form does not have a melting endotherm, so the DSC profile of MNZ-loaded SLM does not show any peaks (Thakkar et al., 2021). The results of the analysis also indicated that MNZ was perfectly encapsulated in the SLM system. To further confirm the solid form of MNZ-loaded SLM, XRD analysis was performed. Based on the analysis results, XRD spectra also show that in pure MNZ, there was a peak in the 13° to 27° area. The appearance of these peaks indicates that MNZ is in the crystalline phase. Still, after being encapsulated in the SLM system, MNZ underwent a transformation to an amorphous phase, which was characterized by a significant decrease in the diffraction peaks on the diffractogram.

3.3. In vitro drug release study

In vitro drug release study was conducted to compare the release profile of pure MNZ (before encapsulation) with MNZ-loaded SLM (MNZ after encapsulation). The drug release profile obtained can be seen in Fig. 3. The figure shows that pure MNZ has a faster release rate than

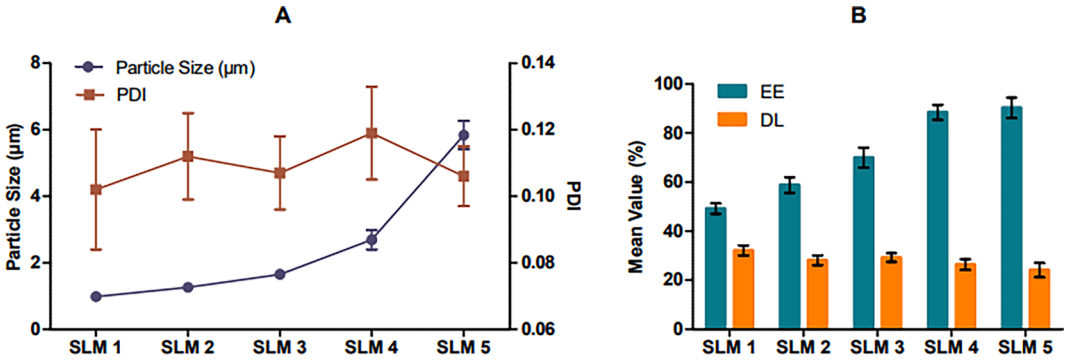

Fig. 1. (A) Particle size, polydispersity index (PDI), (B) entrapment efficiency (EE), and drug loading (DL) of MNZ-loaded SLM (means ± SD, n = 3).

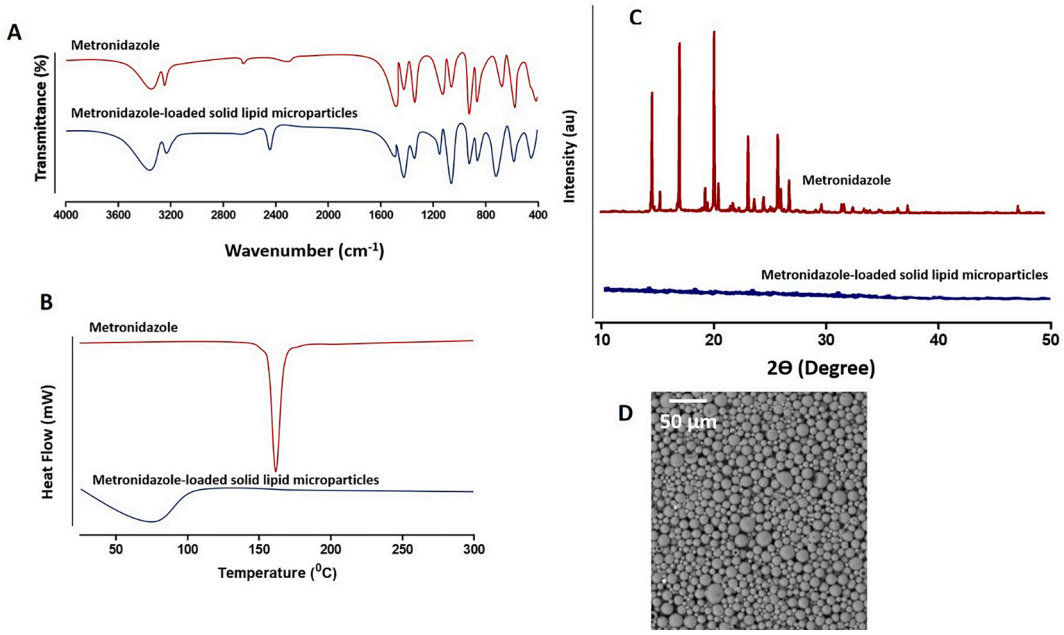

Fig. 2. (A) FTIR spectra, (B) DSC thermogram, and (C) X-ray diffractogram of pure MNZ and optimal MNZ-loaded SLM. (D) SEM image of MNZ-loaded SLM optimal.

MNZ after encapsulation, i.e. after 2 h, the drug has been dissolved in pure drug by 99.18 ± 7.98 %. This was also because pure MNZ has high hydrophilicity, so it can be released in just 2 h (Shinde et al., 2019). Meanwhile, the release rate of MNZ-loaded SLM showed a slower and sustained release, which might be due to the slower diffusion of MNZ encapsulated in the SLM system from the lipid core (Permana et al., 2019). El-Housiny et al. (2018) revealed that the concentration of lipids used in the SLM formulation could affect drug diffusion. As the concentration of lipids increases, the thickness of the lipid matrix in the SLM system also increases, which means an increase in the length of diffusion, which results in a decrease in the rate of drug release.

To understand more about the release mechanism of MNZ-loaded SLM, the release kinetics of MNZ-loaded SLM was evaluated using several mathematical model equations, such as zero order, first order, Higuchi, Korsmeyer-peppes, and Hixson-Crowell. The most appropriate SLM release model was selected based on the highest correlation coefficient (r^2) obtained. Based on the calculation results, this study shows that the Hixson-Crowell release kinetics model is the most appropriate release model that can describe the release of MNZ-loaded SLM, where drug release occurs through dissolution with a constant change in the surface area of the particles (Parmar et al., 2011). This release model usually explains drug release from particles of uniform size (El-say and Hosny, 2018).

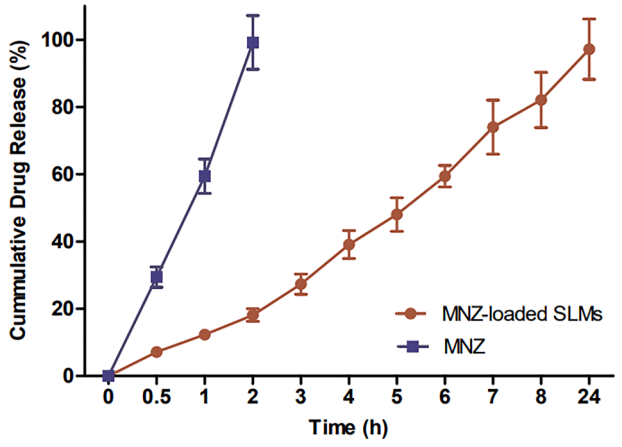

Fig. 3. In vitro release profiles of optimal MNZ-loaded SLM in comparison with the pure MNZ.

3.4. Preparation of SLM-loaded gel

The optimized MNZ-loaded SLM was then incorporated into the gel base. The SLM-loaded gel formulation was made with the aim of increasing the bioavailability of MNZ as well as controlling the release of MNZ on the skin after application. To obtain the optimal SLM-loaded gel formula, this formulation used a variation of the concentration of carbomer: triethanolamine (TEA) namely 0.75 %:1%, 1 %:1.5 %, 1.25 %:1.75 %, and 1.5 %:2% for F1, F2, F3, and F4, respectively. The choice of polymer used is one of the most important factors in the formulation. Carbomer polymers are used as gelling agents. In this study, carbomer was chosen because it has ideal characteristics, such as ease of preparation, and can form gels at low concentrations. This polymer has been widely used in topical formulations (Khurana et al., 2020). Then, other additives used are TEA as an alkalizing agent, which is related to the formation of pH and gel matrix from carbomer through the formation of the polymer chain (Safitri et al., 2021), glycerin as a humectant, DMDM hydantoin as a preservative, and distilled water as a carrier.

3.5. pH, viscosity and rheological examination

The results of determining the pH and viscosity of the SLM-loaded gel can be seen in Table 3. Based on the results of measurements of pH and viscosity of the formulation of the SLM-loaded gel, it shows that the concentration of carbomer has a significant effect ($p < 0.05$) on the pH and viscosity of the gel preparation produced. In each formulation, the pH conditions of the preparations made must be adjusted in such a way according to the conditions at the targeted location so as not to cause irritation and disrupt the function of cell membranes in the body (Luki et al., 2021). The ideal pH value for the skin is in the range of 4 – 7, so the pH of the SLM-loaded gel formulations shows that all formulas have a safe pH that can be accepted by the skin (Lambers et al., 2006). Gel viscosity generally describes the consistency of the gel. It is one of the important parameters in gel formulation because it can affect drug release and extrudability of the gel preparation produced (Ontong et al., 2020). According to Rowe et al. (2009), the viscosity of the polymer

Table 3
Results of pH, viscosity, spreadability, extrudability, and gel strength determination of SLM-loaded gel formulations (means ± SD, n = 3, * = $p < 0.05$).

Formula	pH	Viscosity (mPa.s)	Spreadability (mm)	Extrudability (g/cm^2)	Gel strength (s)
F1	6.74 ± 0.01	24900 ± 1053.57	4.10 ± 0.75	1.54 ± 0.19	38.10 ± 4.14
F2	6.85 ± 0.02	31866.67 ± 65.64*	3.78 ± 0.67	1.49 ± 0.21	40.32 ± 4.31
F3	6.89 ± 0.02	37233.33 ± 1514.38*	3.55 ± 0.63	1.41 ± 0.18	41.98 ± 4.19
F4	6.95 ± 0.02	46766.67 ± 2722.74*	3.31 ± 0.63	1.05 ± 0.17	42.43 ± 4.82

Carbopol 940 (0.5 % w/v) has a viscosity of around 40,000 – 60,000 mPa.s. Thus, the results indicated a decrease in the viscosity of the gelling agent used, which may be due to adding active ingredients and other additives in the formulation. However, the viscosity produced from all SLM-loaded gel formulas still showed good viscosity for topical drug delivery (Ankita et al., 2020; Singh et al., 2013).

Fig. 4 shows the results of the rheological measurements of the SLM-loaded gel formula. It can be seen that the rheogram for formulations F1, F2, and F3 has a pseudoplastic flow type, where there is a decrease in viscosity with an increasing shear rate (rate of share). The curved rheogram in pseudoplastic flow was caused by the interaction between the applied force and the polymer molecules used. As the applied force increases, the polymer molecules, which were normally irregular, would begin to form long chains following the direction of flow. This change in polymer composition would reduce the resistance of the material used and result in a greater change in the shape of the flow at shear stress (Abate and Abel, 2006; Güllü et al., 2020). Meanwhile, the F4 formulation showed a rheogram with a dilatant flow type, where there is a decrease in viscosity by increasing the shear rate (Güllü et al., 2020). Viscosity is influenced by the amount of solute concentration in it. F4 had the highest carbomer concentration, 1.5 %, so it had a higher viscosity, which could cause a dilatant-type flow.

3.6. Spredability test

One aspect of the efficacy of SLM-loaded gel therapy depends on its spread when applied (Ontong et al., 2020). Gels with good spreadability can optimize drug absorption into the skin faster because in the topical application, the high spreadability causes the contact between the drug and the skin to be wider (Safitri et al., 2021). The results of the evaluation of the spreadability of SLM-loaded gel can be seen in Table 3, which showed desired spreadability. It was found that the concentration of carbomer used can affect the spreadability of the gel with significantly different results ($p < 0.05$) between the formulas. The higher the concentration of carbomer, the lower the spreadability produced. This was related to the viscosity obtained; the viscosity is inversely proportional to the spreadability (Aodah et al., 2021). The same results were also obtained in another study using carbomer 940 as a gelling agent with concentrations ranging from 0.5 to 2 %, which showed increasing viscosity and lower spreadability, along with the increasing concentration of carbomer used (Alvionida et al., 2021; Rahmawati and Setiawan, 2019).

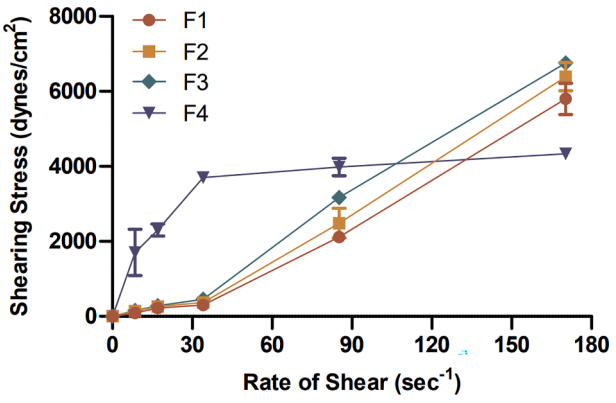

Fig. 4. Rheological examination of SLM-loaded gel.

3.7. Extrudability test

The extrudability test of SLM-loaded gel was carried out to measure how much effort was needed to remove the gel formula from the tube after it was packaged, so that it could facilitate and provide comfort to the patient in its application (Dudhipala and Gorre, 2020; Rajan and Vasudevan, 2012). The test results of the extrudability of the SLM-loaded gel formula can be seen in Table 3. The results showed that the higher the concentration of carbomer used, the lower the extrudability value. It was found that F4 had the lowest extrudability value compared to other formulas, namely 1.05 ± 0.17 g/cm^2, which was significantly different ($p < 0.05$) from other formulations after statistical analysis. This was because carbomer 940 was used as a gelling agent in this study. Thus, the higher the concentration of carbomer used, the lower the extrudability value produced. Carbomers have different characteristics based on their molecular weight. Based on Ojha et al. (2021), carbomer 940 is a polymer with high viscosity characteristics compared to carbomers with other molecular weights, such as carbomers 910 and 941. Thus, high viscosity can increase its consistency in the formulation and provide low extrudability values when used in higher concentrations.

3.8. Gel strength determination

Gel strength in the development of a formulation has become one of the critical parameters that must be considered, especially in its topical application. Before leaching from the target site, a strong gel would support a much greater pressure than a weak gel, thereby preventing rapid drainage of the formulation (Morsi et al., 2017; Priyanka et al., 2019). The results of determining the gel strength of the SLM-loaded gel formulation can be seen in Table 3. Based on the results obtained, it showed that the higher concentration of carbomer used, the stronger the gel strength produced. However, these results showed that the values were not significantly different ($p > 0.05$) between one formula and another after statistical analysis was performed. The value of a good gel strength was in the range of 25 to 50 s. It was previously reported that when the values were below 25 s, the gel produced was too weak and could not maintain its integrity. Therefore, it was easily eroded, whereas if the value was above 50 s, the resulting gel was too stiff and could cause discomfort on the skin surface (Mahajan et al., 2012; Morsi et al., 2017). Accordingly, it can be said that the gel strength between one SLM-loaded gel formula and the other had similarities and was in a good gel strength range.

3.9. In vitro skin occlusivity evaluation

The in vitro skin occlusivity test on the produced SLM gel formulation aimed to increase the ability while maintaining skin hydration characteristics topically (Kenechukwu et al., 2017). The test results can be seen in Fig. 5, which indicated that the incorporation of SLM into the gel in all formulations has a high occlusive value. This was related to the dense nature of the lipid components used in the formulation by clogging the micropores of the filter, thereby preventing water shortages to a greater extent (Kakkar et al., 2018; Mandawgade and Patravale, 2008).

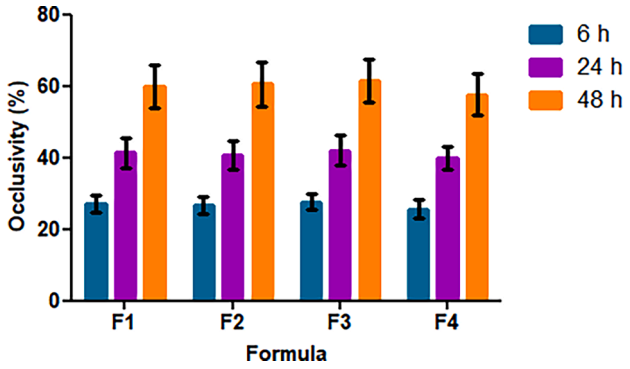

Fig. 5. In vitro skin occlusivity of SLM-loaded gel (means ± SD, n = 3).

Several other studies have also reported comparisons of occlusive skin values obtained between conventional gel formulas with active substances without encapsulation of solid lipids and gels with active substances that have been encapsulated in solid lipids with the same formulation using a carbomer base, showing that ordinary gels with active ingredients without encapsulated solid lipids have a lower occlusive value than gels with active substances that have been encapsulated in solid lipids (Bagde et al., 2019; Kakkar et al., 2018). In addition, the effect of the high occlusiveness of the gel formula used in this rosacea can help the drug penetrate deeper into the skin layer with the gaps between the corneocytes and clog the pores in the skin layer to reduce some of the side effects, such as itching, dryness, and scaling (Bagde et al., 2019; Kenechukwu et al., 2017).

3.10. Ex-vivo skin permeation and retention studies

To determine the effectiveness of the SLM-loaded gel formulation produced and the previously optimized MNZ-loaded SLM in drug delivery, ex vivo permeation, and retention tests were carried out as this study's final proof of concept. The release pattern of MNZ-loaded SLM from the gel was evaluated using a Franz diffusion cell with mouse skin as a diffusion membrane through which the gel would pass. In this study, a gel formulation containing 1 % pure MNZ that was not formulated into the SLM system was used as a control. Fig. 6 (A) and (B) show the cumulative amount and rate of drug release (flux) from the SLM-loaded gel formula through the skin of rats after 24 h. The cumulative amount of MNZ and the permeated drug release rate in formulations F1 to F4 decreased because the higher viscosity values could affect the diffusion rate of the drug to permeate.

Based on the research of Yen et al. (2015), an in vitro drug release test showed that the concentration of carbomer affects drug permeation due to the complexity of the gel network that affects drug diffusion pathways to be absorbed through the membrane. However, the results obtained after statistical analysis showed no significant difference ($p > 0.05$) between formulations F1 and F4. Furthermore, when compared with formulas F1 to F4, the control formula showed the highest cumulative amount of permeated drug with significantly different results ($p < 0.05$). MNZ belongs to BCS class 1, which means it has high permeability and solubility, allowing for higher drug release in the control formula (Zhang et al., 2019). Then the gel formula with encapsulated MNZ showed a slower rate of drug release from formulations F1 to F4. In addition to the effect of carbomer concentration, another thing that might affect drug penetration was the diffusion distance due to the lipid content and high affinity of the drug in the lipid matrix in the SLM system on the gel and the speed of drug partitioning from the lipid phase to the receptor compartment (El-kamel et al., 2007; Rahimpour et al., 2016). Thus, the drug encapsulated in the gel formulation exhibited a slow-release of the drug.

To better understand and correlate the MNZ permeation pattern of the SLM-loaded gel, mathematical modeling kinetics was applied to the release profile of the obtained gel (Tables 4a and 4b). When the correlation coefficient (r^2) values of each kinetic model were compared, all gels were found to exhibit a release pattern behavior following the

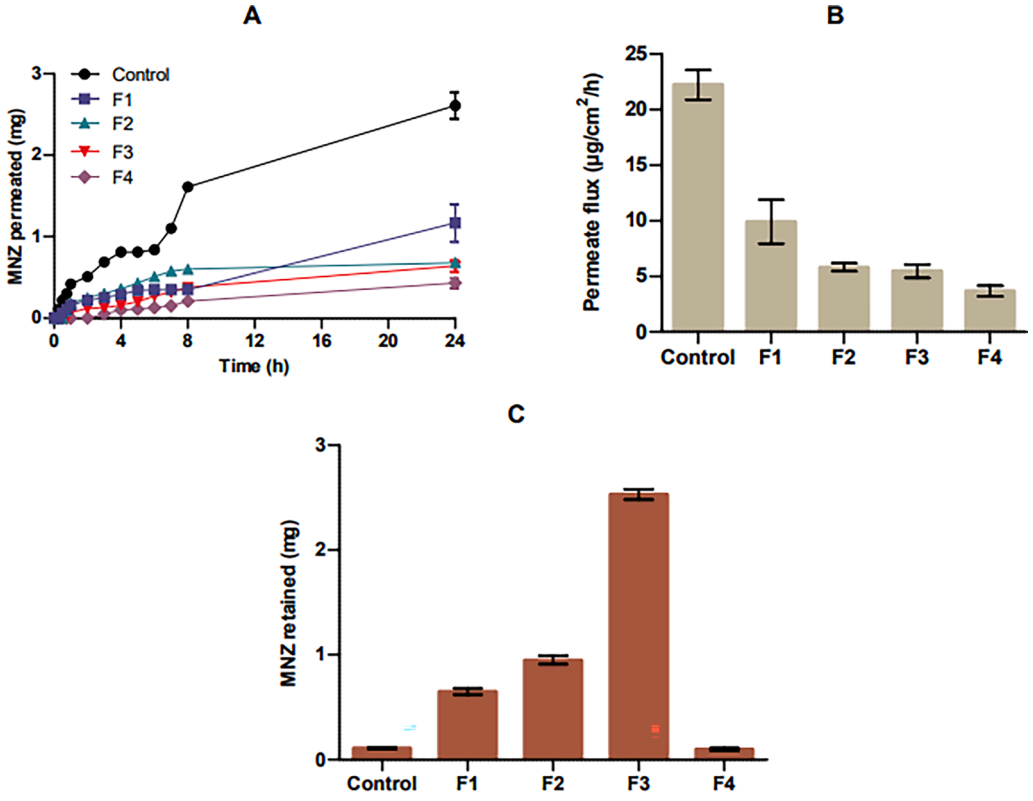

Fig. 6. Results of ex vivo skin permeation (A), permeation flux (B), and retention (C) test of SLM-loaded gel (means ± SD, n = 3).

Table 4a
Mathematical modelling of ex vivo release kinetics parameters.

Formula	Zero-Order		First-Order		Higuchi		Hixson-Crowell		Korsmeyer-Peppas		
	k_0	R^2	k_1	R^2	k_H	R^2	k_{HC}	R^2	k_{KP}	n	R^2
F1	0.509	0.9340	0.005	0.9407	1.770	0.8354	0.002	0.9386	0.848	0.816	0.9642
F2	0.429	0.1900	0.005	0.2379	1.728	0.8501	0.001	0.2219	1.917	0.452	0.8582
F3	0.315	0.8576	0.003	0.8700	1.130	0.8842	0.001	0.8659	0.707	0.707	0.9600
F4	0.191	0.9574	0.002	0.9596	0.642	0.7768	0.001	0.9589	0.251	0.903	0.9649
Control	1.273	0.8049	0.015	0.8654	4.642	0.9162	0.005	0.8470	3.264	0.656	0.9642

Table 4b
Hemolysis persentage of free drug (pure MNZ), MNZ-loaded SLM, and SLM-loaded gel formulations (means ± SD, n = 3).

Concentration (μg/mL)	Hemolysis (%)					
	Free drug	**SLM**	**F1**	**F2**	**F3**	**F4**
500	4.15 ± 0.21	1.09 ± 0.11	3.09 ± 0.29	3.18 ± 0.31	3.21 ± 0.33	3.29 ± 0.35
50	3.18 ± 0.12	0.43 ± 0.02	2.32 ± 0.31	2.29 ± 0.22	2.11 ± 0.21	2.31 ± 0.29
5	2.09 ± 0.13	0.14 ± 0.01	1.02 ± 0.11	1.19 ± 0.12	1.09 ± 0.11	1.22 ± 0.15

Korsmeyer-Peppas kinetic model. The obtained Korsmeyer-Peppas diffusion exponents (n) were 0.816, 0.452, 0.707, 0.903, and 0.656 for F1, F2, F3, F4, and control, respectively. When the diffusion exponents obtained were in the range of 0.45 and 0.89, the F1, F2, F3, and control formulations showed a diffusion anomaly (non-Fickian) which means that the release of MNZ from the SLM-loaded gel occurs through a combination of controlled diffusion and erosion processes. When the value was ≥ 0.89 for the F4 formula, the formula followed the release of MNZ with a super case-II transport mechanism, namely a mechanism controlled by swelling and relaxation of the hydrophilic polymer (Bera et al., 2016; Das et al., 2013; Ignjatović et al., 2021).

One of the goals of the SLM system was to control the release of MNZ and increase its retention time in the skin (Jaspart et al., 2007). Therefore, in this study, a retention test was conducted to determine the ability of SLM-loaded gel to increase drug retention in the skin. Fig. 6 (C) shows the amount of MNZ deposited after 24 h, with formula F3 being the formula with the most MNZ being deposited at 2.53 ± 0.05 mg. Statistical analysis showed a significantly different value ($p < 0.05$) between the F3 formula and other formulas, as well as the control. The higher the carbomer concentration, the greater the amount of MNZ deposited. This was due to an increase in viscosity, which maintained SLM particles in the preparation and slowed down the rate of diffusion of drug molecules to permeate the skin. However, if the viscosity value was too large, it could significantly impact the diffusion rate of drug molecules, resulting in a lower amount of MNZ deposited on F4. Meanwhile, the control formulation containing MNZ, which was not formulated into the SLM system, also resulted in a small amount of MNZ being deposited due to the small molecule of MNZ, making it easier to permeate through the membrane. Based on research by Rahimpour et al. (2016), drugs formulated in the SLM system that was delivered in gel preparations could increase drug retention in the skin. Therefore, MNZ, which was encapsulated in the SLM system and formulated in a gel preparation with a carbomer concentration of 1.25 % (F3), was chosen as the optimal formula with good drug release and retention in delivering the drug topically.

3.11. In vitro hemolysis test of MNZ-loaded SLM and SLM-loaded gel

To assess the safety and irritation potential of the resulting formula, a hemolytic activity test on red blood cells (RBC) was performed. Biomaterials that would be used for direct application to wounds of rosacea sufferers must be compatible with red blood cells so that hemostatic activity is not disturbed. Accordingly, it can adequately help the wound healing process (López-Iglesias et al., 2020). The results of the hemolytic activity test of free drug (pure MNZ), optimal MNZ-loaded SLM, and all SLM-loaded gel formulas showed a low percentage of hemolysis (Tables 4a and 4b). The hemolysis index was considered to be safe when the value was < 5 % (Enggi et al., 2021; Helal et al., 2016). Thus, from the results obtained, it can be concluded that the optimal SLM and the resulting gel were potentially safe and hemocompatible.

3.12. In vitro antioxidant activity

In the clinical manifestations of rosacea, free radicals have been found to play an important role in extrinsic and intrinsic aging. The reactive oxygen species produced by neutrophiles can lead to damage to oxidative tissue (Miyachi, 2001). Accordingly, in this study, we evaluated the antioxidant activity of MNZ. In DPPH evaluations, the IC50 values of free drug, SLM, F1, F2, F3 and F4 were found to be 103.88 ± 9.34 μg/mL, 109.11 ± 10.02 μg/mL, 102.65 ± 8.08 μg/mL, 112.43 ± 11.31 μg/mL, 106.42 ± 11.05 μg/mL and 107.17 ± 9.87 μg/mL, respectively. Furthermore, in the lipid peroxidation method, the IC50 values were 121.03 ± 11.31 μg/mL for free drug, 126.03 ± 11.98 μg/mL for SLM, 131.45 ± 12.01 μg/mL for F1, 126.98 ± 12.01 μg/mL for F2, 131.22 ± 12.15 μg/mL for F3 and 127.87 ± 11.81 μg/mL for F4. In both methods, there were no significant differences ($p > 0.05$) in the IC50 values, indicating that the formulation of MNZ into SLM and hydrogel did not affect the antioxidant properties of MNZ.

4. Conclusion

This study focuses on developing a drug delivery system for treating rosacea with the hydrophilic drug MNZ. MNZ encapsulated in the SLM system has shown excellent quality characteristics with sustained in vitro drug release. The optimal SLM obtained was further developed in the form of a gel dosage form with a carbopol. The carbopol with 1.25 % could provide optimal physical characteristics of the gel and show a better drug release profile, which was significantly different from the control formula and other formulations with the amount of permeated and retained MNZ of 0.64 ± 0.07 mg and 2.53 ± 0.05 mg, respectively. The developed MNZ-loaded SLM and SLM-loaded gel also showed that these formulations were hemocompatible, so they were safe to use in rosacea treatment. In the antioxidant evaluation, the formulation of MNZ into SLM and hydrogel did not affect the property of MNZ in inhibiting free radicals. However, further evaluation of the development of this system needs to be carried out, such as determining the kinetic profile of MNZ release from SLM-loaded gel in vivo using suitable experimental animals, stability testing, and irritation testing of SLM-loaded gel to provide maximum results in the development of MNZ delivery systems for topical rosacea therapy.

CRediT authorship contribution statement

Sulistiawati: Conceptualization, Methodology, Funding acquisition, Writing – original draft. **Kadek Saka Dwipayanti:** Methodology, Writing – original draft. **Muhammad Azhar:** Methodology, Writing –

original draft. **Latifah Rahman:** Methodology, Data curation. **Ermina Pakki:** Methodology, Data curation. **Achmad Himawan:** Data curation, Validation, Supervision. **Andi Dian Permana:** Conceptualization, Project administration, Funding acquisition, Validation, Supervision, Writing – original draft.

Declaration of Competing Interest

The authors declare that they have no known competing financial interests or personal relationships that could have appeared to influence the work reported in this paper.

Data availability

No data was used for the research described in the article.

Acknowledgements

The authors wish to thank Gattefosse Pvt. Ltd., France for providing the lipids.

References

Abate, M., Abel, S.K., 2006. Remington: The Science and Practice of Pharmacy, 21st Edition. Lippincott Williams and Wilkins, Philadelphia.

Agubata, C., Chime, S., Kenechukwu, F., Nzekwe, I., Onunkwo, G., 2014. Formulation and characterization of hydrochlorothiazide solid lipid microparticles based on lipid matrices of Irvingia fat. Int. J. Pharm. Investig. 4, 189–194. https://doi.org/10.4103/2230-973x.143120.

Akki, R., Bhattiprolu, S.S., Vinukonda, A., Kathirvel, S., 2022. An overview on liposheres. World J. Pharm. Res. 11, 217–232. https://doi.org/10.20959/wjpr20228-24470.

Algahtani, M.S., Ahmad, M.Z., Ahmad, J., 2020. Nanoemulsion loaded polymeric hydrogel for topical delivery of curcumin in psoriasis. J. Drug Deliv. Sci. Technol. 59, 101847 https://doi.org/10.1016/j.jddst.2020.101847.

Algul, D., Duman, G., Ozdemir, S., Acar, E.T., Yener, G., 2018. Preformulation, Characterization, and In Vitro Release Studies of Caffeine-Loaded Solid Lipid Nanoparticles. J. Cosmet. Sci. 69, 165–173.

Aliyah, A., Oktaviana, W.W., Dwipayanti, K.S., Erdiana, A.P., Utami, R.N., Permana, A. D., 2021. Enhanced skin localization of doxycycline using microparticles and hydrogel: Effect of oleic acid as penetration enhancer. Pharmaciana 11, 239. 10.12928/pharmaciana.v11i2.21044.

Alvionida, F., Sulistyani, N., Sugihartini, N., 2021. Composition of carbopol 940 and HPMC affects antibacterial activity of beluntas (Pluchea indica (L.)) leaves extract gel. Pharmaciana 11, 427–438. https://doi.org/10.12928/pharmaciana.v11i3.20017.

Ankita, K., Asha, D., Baquee, A.A., 2020. Formulation and evaluation of transdermal topical gel of ibuprofen. J. Drug Deliv. Ther. 10, 20–25.

Aodah, A.H., Bakr, A.A., Booq, R.Y., Rahman, M.J., Alzahrani, D.A., Alsulami, K.A., Alshaya, H.A., Alsuabeyl, M.S., Alyamani, E.J., Tawfik, E.A., 2021. Preparation and evaluation of benzalkonium chloride hand sanitizer as a potential alternative for alcohol-based hand gels. Saudi Pharm. J. https://doi.org/10.1016/j.jsps.2021.06.002.

Badie, H., Abbas, H., 2018. Novel small self-assembled resveratrol -bearing cubosomes and hexosomes: preparation, charachterization and ex vivo permeation. Drug Dev. Ind. Pharm. 10.1080/03639045.2018.1508220.

Bagde, A., Patel, K., Kutlehria, S., Chowdhury, N., Singh, M., 2019. Formulation of topical ibuprofen solid lipid nanoparticle (SLN) gel using hot melt extrusion technique (HME) and determining its anti-inflammatory strength. Drug Deliv. Transl. Res. https://doi.org/10.1007/s13346-019-00632-3.

Bera, H., Gaini, C., Kumar, S., Sarkar, S., Boddupalli, S., Ippagunta, S.R., 2016. HPMC-based gastroretentive dual working matrices coated with Ca+ 2 ion crosslinked alginate-fenugreek gum gel membrane. Mater. Sci. Eng. C 67, 170–181. https://doi.org/10.1016/j.msec.2016.05.016.

Berthet, A., Oltramare, C., Spring, P., Hechon, J., Hopf, N.B., 2020. Human skin permeation rates ex vivo following exposures to mixtures of glycol ethers. Toxicol. Lett. 335, 1–10. https://doi.org/10.1016/j.toxlet.2020.09.017.

Berth-Jones, J., Goh, C.L., Maibach, H.I., 2020. Updates in Clinical Dermatology: Rosacea. Springer Nature Switzerland, USA.

Bertoni, S., Tedesco, D., Bartolini, M., Prata, C., Passerini, N., Albertini, B., 2020. Solid lipid microparticles for oral delivery of catalase: focus on the protein structural integrity and gastric protection. Mol. Pharm. 17, 3609–3621. https://doi.org/10.1021/acs.molpharmaceut.0c00666.

Ceruelos, A.H., Romero-Quezada, L.C., Ruvalcaba Ledezma, J.C., López Contreras, L., 2019. Therapeutic uses of metronidazole and its side effects: An update. Eur. Rev. Med. Pharmacol. Sci. 23, 397–401. https://doi.org/10.26355/eurrev_201901_16788.

Das, B., Nayak, A.K., Nanda, U., 2013. Topical gels of lidocaine HCl using cashew gum and Carbopol 940: Preparation and in vitro skin permeation. Int. J. Biol. Macromol. 62, 514–517. https://doi.org/10.1016/j.ijbiomac.2013.09.049.

de Araújo, J.S.M., Volpato, M.C., Muniz, B.V., Xavier, G.G.A., Martinelli, C.C.M., Lopez, R.F.V., Groppo, F.C., Franz-Montan, M., 2021. Resistivity technique for the evaluation of the integrity of buccal and esophageal epithelium mucosa for in vitro permeation studies : swine buccal and esophageal mucosa barrier models. Pharmaceutics 13, 1–13.

De Caro, V., Giannola, L.I., Di Prima, G., 2021. Solid and semisolid innovative formulations containing miconazole-loaded solid lipid microparticles to promote drug entrapment into the buccal mucosa. Pharmaceutics 13, 1–21. https://doi.org/10.3390/pharmaceutics13091361.

Dolatabadi, J.E.N., Valizadeh, H., Hamishehkar, H., 2015. Solid lipid nanoparticles as efficient drug and gene delivery systems: Recent breakthroughs. Adv. Pharm. Bull. 5, 151–159. 10.15171/apb.2015.022.

Dudhipala, N., Gorre, T., 2020. Neuroprotective effect of ropinirole lipid nanoparticles enriched hydrogel for parkinson's disease: In vitro, ex vivo, pharmacokinetic and pharmacodynamic evaluation. Pharmaceutics 12, 1–24. https://doi.org/10.3390/pharmaceutics12050448.

El-Housiny, S., Eldeen, M.A.S., El-Attar, Y.A., Salem, H.A., Attia, D., Bendas, E.R., El-Nabarawi, M.A., 2018. Fluconazole-loaded solid lipid nanoparticles topical gel for treatment of pityriasis versicolor: Formulation and clinical study. Drug Deliv. 25, 78–90. https://doi.org/10.1080/10717544.2017.1413444.

El-kamel, A.H., Al-fagih, I.M., Alsarra, I.A., 2007. Testosterone solid lipid microparticles for transdermal drug delivery. Formulation and physicochemical characterization. J. Microencapsul. 24, 457–475. https://doi.org/10.1080/02652040701368865.

Elmas, A., Akyüz, G., Bergal, A., Andaç, M., Andaç, Ö., 2020. Mathematical modelling of drug release. Res. Eng. Struct. Mater. 6, 327–350. https://doi.org/10.17515/resm2020.178na0122.

El-say, K.M., Hosny, K.M., 2018. Optimization of carvedilol solid lipid nanoparticles : An approach to control the release and enhance the oral bioavailability on rabbits. PLoS One 1–15.

Enggi, C.K., Isa, H.T., Sulistiawati, S., Ardika, K.A.R., Wijaya, S., Asri, R.M., Mardikasari, S.A., Donnelly, R.F., Permana, A.D., 2021. Development of thermosensitive and mucoadhesive gels of cabotegravir for enhanced permeation and retention profiles in vaginal tissue: A proof of concept study. Int. J. Pharm. 609, 121182 https://doi.org/10.1016/j.ijpharm.2021.121182.

Engin, B., Çiğdem, M., Oba, Ç., Kutlubay, Z., 2017. Acne Rosacea. Acne and Acneiform Eruptions. 183–193. https://doi.org/10.5772/65636.

Ghaderi, S., Ghanbarzadeh, S., Mohammadhassani, Z., Hamishehkar, H., 2014. Formulation of gammaoryzanol-loaded nanoparticles for potential application in fortifying food products. Adv. Pharm. Bull. 4, 549–554. https://doi.org/10.5681/apb.2014.081.

Gonçalves, M.M.B.D.M.M., De Pina, M.E.S.R.T., 2017. Dermocosmetic care for rosacea. Brazilian J. Pharm. Sci. 53, 1–16. https://doi.org/10.1590/s2175-97902017000400182.

Güllü, H., Nuaimi, M.M.D.A., Aytek, A., 2020. Rheological and strength performances of cold-bonded geopolymer made from limestone dust and bottom ash for grouting and deep mixing. Bull. Eng. Geol. Environ.

Hajariwala, N.R., Chandrakar, V.R., Lakhani, J.D., 2021. Peripheral neuropathy : a rare side effect of metronidazole. J. Integr. Heal. Sci. 83–85 https://doi.org/10.4103/JIHS.JIHS.

Helal, H.M., Mortada, S.M., Sallam, M.A., 2016. Paliperidone-loaded nanolipomer system for sustained delivery and enhanced intestinal permeation : superiority to polymeric and solid lipid nanoparticles. AAPS PharmSciTech. https://doi.org/10.1208/s12249-016-0657-1.

Himawan, A., Djide, N.J.N., Mardikasari, S.A., Utami, R.N., Arjuna, A., Donnelly, R.F., Permana, A.D., 2022. A novel in vitro approach to investigate the effect of food intake on release profile of valsartan in solid dispersion-floating gel in-situ delivery system. Eur. J. Pharm. Sci. 168, 106057 https://doi.org/10.1016/j.ejps.2021.106057.

Ignjatović, J., Đuriš, J., Cvijić, S., Dobričić, V., Montepietra, A., Lombardi, C., Ibrić, S., Rossic, A.A., 2021. Development of solid lipid microparticles by melt-emulsification/spray- drying processes as carriers for pulmonary drug delivery. Eur. J. Pharm. Sci. 156.

Jabbehdari, S., Memar, O.M., Caughlin, B., Djalilian, A.R., 2021. Update on the pathogenesis and management of ocular rosacea: an interdisciplinary review Sayena. Eur. J. Ophthalmol. 31, 22–33. https://doi.org/10.1177/1120672120937252.

Jaspart, S., Pascal, B., Piel, G., Dogné, J.-M., Delattre, L., Evrard, B., 2007. Solid lipid microparticles as a sustained release system for pulmonary drug delivery. Eur. J. Pharm. Biopharm. 65, 47–56. 10.1016/j.ejpb.2006.07.006.

Kakkar, V., Kaur, I.P., Kaur, A.P., Saini, K., Singh, K.K., 2018. Topical delivery of tetrahydrocurcumin lipid nanoparticles effectively inhibits skin inflammation: in vitro and in vivo study. Drug Dev. Ind. Pharm. https://doi.org/10.1080/03639045.2018.1492607.

Kaur, R., Ajitha, M., 2019. Formulation of transdermal nanoemulsion gel drug delivery system of lovastatin and its in vivo characterization in glucocorticoid induced osteoporosis rat model. J. Drug Deliv. Sci. Technol. https://doi.org/10.1016/j.jddst.2019.06.008.

Kaur, L.P., Guleri, T.K., 2013. Topical gel: a recent approach for novel drug delivery. Asian J. Biomed. Pharm. Sci. 3, 1–5.

Kazemi, D., Salouti, M., Rostamizadeh, K., Zabihian, A., 2014. Development of gentamicin-loaded solid lipid nanoparticles : evaluation of drug release kinetic and antibacterial activity against staphylococcus aureus development of gentamicin-loaded solid lipid nanoparticles : evaluation of drug release kinetic and an. Int. J. Pharm. Res. Innov. 7, 1–6.

Kenechukwu, F.C., Attama, A.A., Ibezim, E.C., Nnamani, P.O., Umeyor, C.E., Uronnachi, E.M., Gugu, T.H., Momoh, M.A., Ofokansi, K.C., Akpa, P.A., 2017. Surface-modified mucoadhesive microgels as a controlled release system for

miconazole nitrate to improve localized treatment of vulvovaginal candidiasis. Eur. J. Pharm. Sci. https://doi.org/10.1016/j.ejps.2017.10.002.
Khurana, B., Arora, D., Narang, R.K., 2020. QbD based exploration of resveratrol loaded polymeric micelles based carbomer gel for topical treatment of plaque psoriasis: In vitro, ex vivo and in vivo studies. J. Drug Deliv. Sci. Technol. https://doi.org/10.1016/j.jddst.2020.101901.
Khurana, S., Jain, N.K., Bedi, P.M.S., 2013. Development and characterization of a novel controlled release drug delivery system based on nanostructured lipid carriers gel for meloxicam. Life Sci. 93, 763–772. https://doi.org/10.1016/j.lfs.2013.09.027.
Lambers, H., Piessens, S., Bloem, A., Pronk, H., Finkel, P., 2006. Natural skin surface pH Is on average below 5, which is beneficial for its resident flora Natural skin surface pH is on average below 5, which is beneficial for its resident flora. Int. J. Cosmet. Sci. 28, 359–370. https://doi.org/10.1111/j.1467-2494.2006.00344.x.
López-Iglesias, C., Barros, J., Ardao, I., Gurikov, P., Monteiro, F.J., Smirnova, I., Alvarez-Lorenzo, Carmen García-González, C.A., 2020. Jet Cutting Technique for the Production of Chitosan Aerogel Microparticles Loaded with Vancomycin. Polymers (Basel). 12, 1–13.
Luki, M., Pantelic, I., Savi, S.D., 2021. Towards Optimal pH of the Skin and Topical Formulations : From the Current State of the Art to Tailored Products. Cosmetics 8.
Lv, Y., He, H., Qi, J., Lu, Y.i., Zhao, W., Dong, X., He, H., Qi, J., Lu, Y., Zhao, W., Dong, X., Wu, W., 2018. Visual validation of the measurement of entrapment efficiency of. Int. J. Pharm. https://doi.org/10.1016/j.ijpharm.2018.06.025.
Mahajan, H.S., Tyagi, V., Lohiya, G., Nerkar, P., 2012. Thermally reversible xyloglucan gels as vehicles for Th nasal drug delivery. Drug Deliv. 19, 270–276. https://doi.org/10.3109/10717544.2012.704095.
Malik, D.S., Kaur, G., 2018. Nanostructured gel for topical delivery of azelaic acid: Designing, characterization, and in-vitro evaluation. J. Drug Deliv. Sci. Technol. 47, 123–136.
Mandawgade, S.D., Patravale, V.B., 2008. Development of SLNs from natural lipids: Application to topical delivery of tretinoin. Int. J. Pharm. 363, 132–138. https://doi.org/10.1016/j.ijpharm.2008.06.028.
Mirchandani, Y., Patravale, V.B., Brijesh, S., 2021. Solid lipid nanoparticles for hydrophilic drugs. J. Control. Release 335, 457–464. https://doi.org/10.1016/j.jconrel.2021.05.032.
Miyachi, Y., 2001. Potential antioxidant mechanism of action for metronidazole: Implications for rosacea management. Adv. Ther. 18, 237–243. https://doi.org/10.1007/BF02850193.
Miyachi, Y., Yamasaki, K., Fujita, T., Fujii, C., 2022. Metronidazole gel (0. 75 %) in Japanese patients with rosacea : A randomized, vehicle- - controlled, phase 3 study. J. Dermatology 49, 330–340. https://doi.org/10.1111/1346-8138.16254.
Morsi, N., Ibrahim, M., Refai, H., El Sorogy, H., 2017. Nanoemulsion-based electrolyte triggered in situ gel for ocular delivery of acetazolamide. Eur. J. Pharm. Sci. 104, 302–314. https://doi.org/10.1016/j.ejps.2017.04.013.
Mu, H., Holm, R., 2018. Solid lipid nanocarriers in drug delivery: characterization and design. Expert Opin. Drug Deliv. https://doi.org/10.1080/17425247.2018.1504018.
Nabi-Meibodi, M., Navidi, B., Navidi, N., Vatanara, A., Reza Rouini, M., Ramezani, V., 2013. Optimized double emulsion-solvent evaporation process for production of solid lipid nanoparticles containing baclofene as a lipid insoluble drug. J. Drug Deliv. Sci. Technol. 23, 225–230. https://doi.org/10.1016/S1773-2247(13)50034-7.
Nahum, V., Domb, A.J., 2021. Recent developments in solid lipid microparticles for food ingredients delivery. Foods 10, 1–25. https://doi.org/10.3390/foods10020400.
Neupane, R., Boddu, S.H.S., Renukuntla, J., Babu, R.J., 2020. Alternatives to biological skin in permeation studies : current trends and possibilities. Pharmaceutics 12.
Ojha, B., Kumar, V., Surabhi, J., Sushama, G., 2021. Nanoemulgel : a promising novel formulation for treatment of skin ailments. Polym. Bull. https://doi.org/10.1007/s00289-021-03729-3.
Ontong, J.C., Singh, S., Nwabor, O.F., Chusri, S., Voravuthikunchai, S.P., 2020. Potential of antimicrobial topical gel with synthesized biogenic silver nanoparticle using Rhodomyrtus tomentosa leaf extract and silk sericin. Biotechnol. Lett. https://doi.org/10.1007/s10529-020-02971-5.
Oriani, V.B., Alvim, I.D., Consoli, L., Molina, G., Pastore, G.M., Hubinger, M.D., 2016. Solid lipid microparticles produced by spray chilling technique to deliver ginger oleoresin: Structure and compound retention. Food Res. Int. 80, 41–49. https://doi.org/10.1016/j.foodres.2015.12.015.
Parmar, B., Mandal, S.A., Petkar, K.C., Patel, L.D., Sawant, K.K., 2011. Valsartan Loaded Solid Lipid Nanoparticles: Development, Characterization, and In vitro and Ex vivo Evaluation. Int. J. Pharm. Sci. Nanotechnol. 4, 1483–1490. 10.37285/ijpsn.2011.4.3.7.
Patel, J., Patel, B., Banwit, H., Parmar, K., Patel, M., 2011. Formulation and evaluation of topical aceclofenac gel using different gelling agent. Int. J. Drug Dev. Res. 3, 156–164.
Patil, P.B., Datir, S.K., Saudagar, R.B., 2019. A review on topical gels as drug delivery system. J. Drug Deliv. Ther. 9, 989–994.
Permana, A.D., Anjani, Q.K., Sartini, Utomo, E., Volpe-Zanutto, F., Paredes, A.J., Evary, Y.M., Mardikasari, S.A., Pratama, M.R., Tuany, I.N., Donnelly, R.F., 2021a. Selective delivery of silver nanoparticles for improved treatment of biofilm skin infection using bacteria-responsive microparticles loaded into dissolving microneedles. Mater. Sci. Eng. C 120, 111786.
Permana, A.D., Tekko, I.A., McCrudden, M.T.C., Anjani, Q.K., Ramadon, D., McCarthy, H.O., Donnelly, R.F., 2019. Solid lipid nanoparticle-based dissolving microneedles: A promising intradermal lymph targeting drug delivery system with potential for enhanced treatment of lymphatic filariasis. J. Control. Release 316, 34–52.
Permana, A.D., Paredes, A.J., Volpe-Zanutto, F., Anjani, Q.K., Utomo, E., Donnelly, R.F., 2020a. Dissolving microneedle-mediated dermal delivery of itraconazole nanocrystals for improved treatment of cutaneous candidiasis. Eur. J. Pharm. Biopharm. 154, 50–61. https://doi.org/10.1016/j.ejpb.2020.06.025.
Permana, A.D., Utami, R.N., Courtenay, A.J., Manggau, M.A., Donnelly, R.F., Rahman, L., 2020b. Phytosomal nanocarriers as platforms for improved delivery of natural antioxidant and photoprotective compounds in propolis: An approach for enhanced both dissolution behaviour in biorelevant media and skin retention profiles. J. Photochem. Photobiol. B Biol. https://doi.org/10.1016/j.jphotobiol.2020.111846.
Permana, A.D., Utomo, E., Pratama, M.R., Amir, M.N., Anjani, Q.K., Mardikasari, S.A., Sumarheni, S., Himawan, A., Arjuna, A., Usmanengsi, U., Donnelly, R.F., 2021b. Bioadhesive-thermosensitive in situ vaginal gel of the gel flake-solid dispersion of itraconazole for enhanced antifungal activity in the treatment of vaginal candidiasis. ACS Appl. Mater. Interfaces 13, 18128–18141. https://doi.org/10.1021/acsami.1c03422.
Priyanka, N.V.S.A.I., Neeraja, P., Mangilal, T., Kumar, M.R., 2019. Formulation and evaluation of gel loaded with microspheres of apremilast for transdermal delivery system. Asian J. Pharm. Clin. Res. 12. 10.22159/ajpcr.2019.v12i2.29374.
Rabima, R., Sari, M.P., 2019. Entrapment efficiency and drug loading of curcumin nanostructured lipid carrier (NLC) formula. Pharmaciana 9, 299–306. https://doi.org/10.12928/pharmaciana.v9i2.13070.
Rahimpour, Y., Javadzadeh, Y., Hamishehkar, H., 2016. Solid lipid microparticles for enhanced dermal delivery of tetracycline HCl. Colloids Surfaces B Biointerfaces 145, 14–20. https://doi.org/10.1016/j.colsurfb.2016.04.034.
Rahmawati, D.A., Setiawan, I., 2019. The formulation and physical stability test of gel fruit strawberry extract (Fragaria x ananassa Duch.). J. Nutraceuticals Herb. Med. 2, 38–46.
Rainer, B.M., Thompson, K.G., Antonescu, C., Florea, L., Mongodin, E.F., Bui, J., Fischer, A.H., Pasieka, H.B., Garza, L.A., Kang, S., Chien, A.L., 2019. Characterization and analysis of the skin microbiota in rosacea : a case – control study. Am. J. Clin. Dermatol. https://doi.org/10.1007/s40257-019-00471-5.
Rajan, R., Vasudevan, D.T., 2012. Effect of permeation enhancers on the penetration mechanism of transfersomal gel of ketoconazole. J. Adv. Pharm. Tech. Res. 3 https://doi.org/10.4103/2231-4040.97286.
Rowe, R.C., Sheskey, P.J., Quinn, M., 2009. Handbook of Pharmaceutical Excipients, 6th Edition. Pharmaceutical Press and American Pharmacists Association, London.
Safitri, I., Nawangsari, D., Febrina, D., 2021. Overview : application of carbopol 940 in gel. Adv. Heal. Sci. Res. 34, 80–84.
Shi, L., Li, Z., Yu, L., Jia, H., Zheng, L., 2011. Effects of surfactants and lipids on the preparation of solid lipid nanoparticles using double emulsion method. J. Dispers. Sci. Technol. 32, 254–259. https://doi.org/10.1080/01932691003659130.
Shinde, U.A., Parmar, S.J., Easwaran, S., 2019. Metronidazole-loaded nanostructured lipid carriers to improve skin deposition and retention in the treatment of rosacea. Drug Dev. Ind. Pharm. https://doi.org/10.1080/03639045.2019.1569026.
Singh, V.K., Singh, P.K., Sharma, P.K., Srivastava, P.K., Mishra, A., 2013. Formulation and evaluation of topical gel of acelofenac containing piparine. Indo Am. J. PPharmaceutical Res.
Soute, E.B., Müller, R.H., 2007. Lipid nanoparticles (solid lipid nanoparticles and nanostructured lipid carriers) for cosmetic, dermal, and transdermal applications, in: Nanoparticulate Drug-Delivery Systems. pp. 213–229.
Sulistiawati, Enggi, C.K., Isa, H.T., Wijaya, S., Ardika, K.A.R., Asri, R.M., Donnelly, R.F., Permana, A.D., 2021. Validation of spectrophotometric method to quantify cabotegravir in simulated vaginal fluid and porcine vaginal tissue in ex vivo permeation and retention studies from thermosensitive and mucoadhesive gels. Spectrochim. Acta - Part A Mol. Biomol. Spectrosc. 267. 10.1016/j.saa.2021.120600.
Thakkar, R., Jara, M.O., Swinnea, S., Pillai, A.R., Maniruzzaman, M., 2021. Impact of laser speed and drug particle size on selective laser sintering 3d printing of amorphous solid dispersions. Pharmaceutics 13, 1–19. https://doi.org/10.3390/pharmaceutics13081149.
Tran, M.L., Fu, C.C., Juang, R.S., 2019. Effects of water matrix components on degradation efficiency and pathways of antibiotic metronidazole by UV/TiO2 photocatalysis. J. Mol. Liq. https://doi.org/10.1016/j.molliq.2018.11.155.
van Zuuren, E.J., Arents, B.W.M., van der Linden, M.M.D., Vermeulen, S., Fedorowicz, Z., Tan, J., 2021. Rosacea: New Concepts in Classification and Treatment. Am. J. Clin. Dermatol. 22, 457–465. https://doi.org/10.1007/s40257-021-00595-7.
Weiss, E., Katta, R., 2017. Diet and rosacea: the role of dietary change in the management of rosacea. Dermatol. Pract. Concept. 7, 31–37. https://doi.org/10.5826/dpc.0704a08.
Wolska, E., Brach, M., 2022. Distribution of Drug Substances in Solid Lipid Microparticles (SLM)—Methods of Analysis and Interpretation. Pharmaceutics 14, 1–18. https://doi.org/10.3390/pharmaceutics14020335.
Yen, W.F., Basri, M., Ahmad, M., Ismail, M., 2015. Formulation and evaluation of galantamine gel as drug reservoir in transdermal patch delivery system. Sci. World J. 1–7.
Yu, M., Ma, H., Lei, M., Li, N., Tan, F., 2014. In vitro / in vivo characterization of nanoemulsion formulation of metronidazole with improved skin targeting and anti-rosacea properties. Eur. J. Pharm. Biopharm. https://doi.org/10.1016/j.ejpb.2014.03.019.
Zhang, L., Huang, T., Bi, J., Zheng, Y., Lu, C., Hui, Q., 2020. Long-term toxicity study of topical administration of a highly-stable rh-aFGF Carbomer 940 hydrogel in a rabbit skin wound model 11, 1–8. 10.3389/fphar.2020.00058.
Zhang, S., Fang, M., Zhang, Q., Li, X., Zhang, T., 2019. Evaluating the bioequivalence of metronidazole tablets and analyzing the effect of in vitro dissolution on in vivo

absorption based on PBPK modeling. Drug Dev. Ind. Pharm. https://doi.org/10.1080/03639045.2019.1648502.
Zhang, Y., Huo, M., Zhou, J., Zou, A., Li, W., Yao, C., Xie, S., 2010. DDSolver: An add-in program for modeling and comparison of drug dissolution profiles. AAPS J. 12, 263–271.
Zhang, H., Tang, K., Wang, Y., Fang, R., 2021. Rosacea treatment : review and update. Dermatol. Ther. (Heidelb) 11, 13–24. https://doi.org/10.1007/s13555-020-00461-0.